Inexact IETI-DP for conforming isogeometric multi-patch discretizations

Rainer Schneckenleitner* and Stefan Takacs†

Abstract

In this paper, we investigate Dual-Primal Isogeometric Tearing and Interconnecting (IETI-DP) methods for conforming Galerkin discretizations on multi-patch computational domains with inexact subdomain solvers. Recently, the authors have proven a condition number estimate for a IETI-DP solver that is explicit, among other parameters, in the grid size and the spline degree. The analysis assumes that the local subproblems are solved exactly, e.g., using a direct solver. In the present paper, we change the method in order to allow inexact solvers for the local subproblems, namely solvers based on the fast diagonalization method. This gives a faster overall solver, maintaining the same explicit condition number bound.

1 Introduction

We are interested in a fast solver for linear systems that are obtained from the discretization of boundary value problems using Isogeometric Analysis (IgA; [5]) schemes. We consider computational domains that are composed of multiple non-overlapping patches, for which FETI-DP type algorithms are a canonical choice. Adaptations of FETI-DP, introduced in [2], have already been made to IgA, see, e.g., [7, 3]. This approach is sometimes called Dual-Primal Isogeometric Tearing and Interconnecting (IETI-DP) method. Recently, a convergence analysis for IETI-DP methods that is explicit in the grid sizes, the patch diameters, the spline degree and other parameters like the smoothness of the splines within the patches or the number of patches was carried out for a conforming Galerkin IgA discretization, see [10]. There, the authors considered a Schur complement IETI-DP method, where the subdomain problems are solved with sparse direct solvers. In case of large subdomain problems, direct solvers slow down the overall algorithm and require a lot of memory resources. The saddle

*Tampere University, rainer.schneckenleitner@tuni.fi, Corresponding author
†Johannes Kepler University Linz, stefan.takacs@numa.uni-linz.ac.at

point formulation of IETI-DP allows the use of inexact local solvers. The successful use of inexact solvers for FETI-DP has already been demonstrated in [4, 6]. In this paper, we use the fast diagonalization (FD) method introduced in [9] to construct solvers for the local subproblems. We show that the inexact IETI-DP version satisfies the same condition number bound as the IETI-DP solver from [10].

The structure of the paper is as follows. Section 2 is devoted to the introduction of the model problem and the IETI-DP solver. In Section 3, we give a condition number estimate of the preconditioned system. Numerical results are presented in Section 4.

2 Model problem and its solution

Let $\Omega \subset \mathbb{R}^2$ be an open and bounded Lipschitz domain with boundary $\partial\Omega$ and $f \in L_2(\Omega)$ be a given source function. We consider the following model problem: Find $u \in H_0^1(\Omega)$ such that

$$\int_\Omega \nabla u \cdot \nabla v \, \mathrm{d}x = \int_\Omega f v \, \mathrm{d}x \qquad \text{for all } v \in H_0^1(\Omega). \tag{1}$$

We assume that Ω is composed of K non-overlapping patches $\Omega^{(k)}$ that are parameterized with geometry mappings

$$G_k : \widehat{\Omega} := (0,1)^d \to \Omega^{(k)} := G_k(\widehat{\Omega}),$$

where any two patches with non-empty intersection share either a common vertex or a common edge, cf. [10, Ass. 2]. Additionally, we assume that the number of patches sharing a vertex is uniformly bounded, cf. [10, Ass. 3]. Moreover, we assume that there is a constant C_G such that

$$\|\nabla G_k\|_{L_\infty(\widehat{\Omega})} \le C_G \, H_k \quad \text{and} \quad \|(\nabla G_k)^{-1}\|_{L_\infty(\widehat{\Omega})} \le C_G \, H_k^{-1}, \tag{2}$$

where $H_k := \operatorname{diam}(\Omega^{(k)})$ is the patch size, see [10, Ass. 1]. The local discretization spaces on the parameter domain $\widehat{\Omega}$ are tensor-product B-splines spaces of degree p with bases obtained using the Cox-de Boor formula. We assume that these spaces are based on quasi-uniform grids with sizes $\widehat{h}_k$, see [10, Ass. 4]. The local discretization spaces on the physical patches $\Omega^{(k)}$ are obtained by the pull-back principle. The quantity $h_k := H_k \widehat{h}_k$ measures the grid size on the physical domain. We assume that the geometry mappings as well as the discretizations agree on all interfaces between patches, cf. [10, Ass. 5]. So, we are able to set up a fully matching discretization with the function space

$$V = \{v \in H_0^1(\Omega) : v \circ G_k \text{ is a B-spline function}\} \cap C(\Omega).$$

The corresponding discrete problem is obtained by restricting the variational problem (1) to this space.

In the following, we introduce the IETI-DP solver. The patches from the definition of the computational domain provide a canonical choice of substructures which we use to set up the solver. By assembling the variational problem (1) on the patches separately, we obtain yet uncoupled local systems

$$A^{(k)}\underline{u}^{(k)} = \underline{f}^{(k)} \quad \text{for} \quad k = 1, \dots, K,$$

where $A^{(k)}$ is the local stiffness matrix and $\underline{f}^{(k)}$ is the local source vector.

Following the DP approach, we need to select a set of primal degrees of freedom. We restrict ourselves to choosing the function values at the corners of the patches as primal degrees of freedom, see [10, Alg. A]. By splitting of the degrees of freedom into the corner values (index C) and the remaining degrees of freedom (index Δ), we obtain

$$A^{(k)} = \begin{pmatrix} A^{(k)}_{CC} & A^{(k)}_{C\Delta} \\ A^{(k)}_{\Delta C} & A^{(k)}_{\Delta\Delta} \end{pmatrix}, \quad \underline{u}^{(k)} = \begin{pmatrix} \underline{u}^{(k)}_C \\ \underline{u}^{(k)}_\Delta \end{pmatrix}, \quad \underline{f}^{(k)} = \begin{pmatrix} \underline{f}^{(k)}_C \\ \underline{f}^{(k)}_\Delta \end{pmatrix}. \tag{3}$$

As local spaces, we choose the patch-local functions where the corner values vanish, so the still uncoupled local systems are

$$A^{(k)}_{\Delta\Delta}\underline{u}^{(k)}_{\Delta\Delta} = \underline{f}^{(k)}_{\Delta\Delta} \quad \text{for} \quad k = 1, \dots, K. \tag{4}$$

Moreover, we need a primal space spanned by energy minimizing basis functions that form a nodal basis for the primal degrees of freedom. This basis is represented by the matrix $\Psi^{(k)}$ that is characterized by the linear system

$$\underbrace{\begin{pmatrix} A^{(k)} & (C^{(k)})^\top \\ C^{(k)} & \end{pmatrix}}_{=:\,\widetilde{\mathcal{A}}^{(k)}} \begin{pmatrix} \Psi^{(k)} \\ \Delta^{(k)} \end{pmatrix} = \begin{pmatrix} 0 \\ R^{(k)}_c \end{pmatrix}, \tag{5}$$

where $C^{(k)} = (C^{(k)}_C, C^{(k)}_\Delta) = (I, 0)$ is a matrix that represents the evaluation of the primal degrees of freedom and $R^{(k)}_c$ is a binary local-to-global mapping that identifies the local ordering of the primal degrees of freedom and their global ordering. We compute $\Psi^{(k)}$ by solving (5) using a MINRES solver, preconditioned with

$$\widetilde{P}^{(k)} = \begin{pmatrix} (\widehat{A}^{(k)}_M)^{-1} & \\ & (C^{(k)}(\widehat{A}^{(k)}_M)^{-1}C^{(k)})^{-1} \end{pmatrix},$$

where

$$\widehat{A}^{(k)}_M := \widehat{A}^{(k)} + \gamma_k \widehat{M}^{(k)} \underline{e}^{(k)}_h (\underline{e}^{(k)}_h)^\top \widehat{M}^{(k)},$$

$\widehat{A}^{(k)}$ is the stiffness matrix on the parameter domain (obtained from discretizing $\int_{\widehat{\Omega}} \nabla\widehat{u} \cdot \nabla\widehat{v}\,\mathrm{d}x$), $\widehat{M}^{(k)}$ is the analogously defined mass matrix and $\underline{e}^{(k)}_h$ represents the constant function with value 1. We choose $\gamma_k = 1$ if $\Omega^{(k)}$ does not contribute to the Dirichlet boundary $\partial\Omega$ and $\gamma_k = 0$ otherwise. The application of $(\widehat{A}^{(k)}_M)^{-1}$ is realized with the

fast diagonalization (FD) method, see [9]. After the computation of all matrices $\Psi^{(k)}$, we obtain the global primal basis representation matrix Ψ by canonical mappings.

To ensure continuity, we introduce jump matrices $B^{(k)}$, where the condition $\sum_{k=1}^{K} B^{(k)}\underline{u}^{(k)} = 0$ holds if and only if the basis functions are continuous between the patches (except the continuity at the corners), in the usual way, see [10, Section 3]. The matrices $B_\Delta^{(k)}$ are obtained from $B^{(k)}$ again by eliminating the entries corresponding to the primal degrees of freedom.

The overall IETI-DP saddle point system is obtained by coupling the local systems (4) and the primal system using the jump matrices and reads as follows:

$$\begin{pmatrix} A_{\Delta\Delta}^{(1)} & & & & (B_\Delta^{(1)})^\top \\ & \ddots & & & \vdots \\ & & A_{\Delta\Delta}^{(K)} & & (B_\Delta^{(K)})^\top \\ & & & A_\Pi & B_\Pi^\top \\ B_\Delta^{(1)} & \cdots & B_\Delta^{(K)} & B_\Pi & 0 \end{pmatrix} \begin{pmatrix} \underline{u}_\Delta^{(1)} \\ \vdots \\ \underline{u}_\Delta^{(K)} \\ \underline{u}_\Pi \\ \underline{\lambda} \end{pmatrix} = \begin{pmatrix} \underline{f}_\Delta^{(1)} \\ \vdots \\ \underline{f}_\Delta^{(K)} \\ \underline{f}_\Pi \\ 0 \end{pmatrix}, \tag{6}$$

where

$$A_\Pi := \sum_{k=1}^{K} (\Psi^{(k)})^\top A^{(k)} \Psi^{(k)}, \quad \underline{f}_\Pi := \Psi^\top \underline{f} \quad \text{and} \quad B_\Pi := \sum_{k=1}^{K} B^{(k)} \Psi^{(k)}.$$

We solve (6) with a MINRES solver, preconditioned with

$$\mathcal{P} := \operatorname{diag}\,(P, A_\Pi^{-1}, \widehat{M}_{\mathrm{sD}}), \tag{7}$$

where $P := \operatorname{diag}\,(P^{(1)}, \cdots, P^{(K)})$ and $P^{(k)} := Q^{(k)} (\widehat{A}_M^{(k)})^{-1} (Q^{(k)})^\top$ and $Q^{(k)} := (A_{\Delta\Delta}^{-1} A_{\Delta C}, I)$ is the $A^{(k)}$-orthogonal projection from the local function space into the space of functions with vanishing corner values; its entries can be extracted from $\Psi^{(k)} = (I, -((A_{\Delta\Delta}^{(k)})^{-1} A_{\Delta C}^{(k)})^\top)^\top R_c$. The matrix $\widehat{A}_M^{(k)}$ is defined as above and realized using the FD method. A_Π^{-1} is realized using a direct solver. For the setup of the inexact scaled Dirichlet preconditioner $\widehat{M}_{\mathrm{sD}}$, we define analogously to (3) a splitting into basis functions vanishing at the interfaces (index I) and remaining basis functions (index Γ). Then, we define

$$\widehat{M}_{\mathrm{sD}} := B_\Gamma D^{-1} \widehat{S} D^{-1} B_\Gamma^\top,$$

where $\widehat{S} := \operatorname{diag}(\widehat{S}^{(1)}, \ldots, \widehat{S}^{(K)})$ with $\widehat{S}^{(k)} := \widehat{A}_{\Gamma\Gamma}^{(k)} - \widehat{A}_{\Gamma I}^{(k)} (\widehat{A}_{II}^{(k)})^{-1} \widehat{A}_{I\Gamma}^{(k)}$. The diagonal matrix D is based on the principle of multiplicity scaling, cf. [10]. The application of $(\widehat{A}_{II}^{(k)})^{-1}$ is also realized using the FD method.

3 Analysis of the method

3.1 Analysis of the main iteration

First, we show that the chosen preconditioners for the local problems are optimal up to constants.

Lemma 3.1. *The preconditioner* $P^{(k)} = Q^{(k)}(\widehat{A}_M^{(k)})^{-1}(Q^{(k)})^\top$ *is spectrally equivalent to the matrix* $(A_{\Delta\Delta}^{(k)})^{-1}$*, i.e.,* $P^{(k)} \eqsim (A_{\Delta\Delta}^{(k)})^{-1}$.

Proof. We show the equivalent statement $A_{\Delta\Delta}^{(k)} P^{(k)} A_{\Delta\Delta}^{(k)} \eqsim A_{\Delta\Delta}^{(k)}$. Since we assume (2), [10, Lemma 4.13] yields $A^{(k)} \eqsim \widehat{A}^{(k)}$. From this observation, the desired result follows immediately if $\partial\Omega^{(k)} \cap \partial\Omega \neq \emptyset$. For the case $\partial\Omega^{(k)} \cap \partial\Omega = \emptyset$, we define $\underline{e}_h$ be the vector representing the constant function with value 1. Due to the definitions of $P^{(k)}$, the $A^{(k)}$-orthogonal projection $Q^{(k)}$, we get using the norm equivalence, [10, Lemma 4.13], that

$$\begin{aligned}
A_{\Delta\Delta}^{(k)} P^{(k)} A_{\Delta\Delta}^{(k)} &= A_{\Delta\Delta}^{(k)} Q^{(k)} (\widehat{A}^{(k)} + \widehat{M}^{(k)} \underline{e}_h \underline{e}_h^\top \widehat{M}^{(k)})^{-1} (Q^{(k)})^\top A_{\Delta\Delta}^{(k)} \\
&= \begin{pmatrix} A_{\Delta C}^{(k)} & A_{\Delta\Delta}^{(k)} \end{pmatrix} (\widehat{A}^{(k)} + \widehat{M}^{(k)} \underline{e}_h \underline{e}_h^\top \widehat{M}^{(k)})^{-1} \begin{pmatrix} A_{C\Delta}^{(k)} \\ A_{\Delta\Delta}^{(k)} \end{pmatrix} \\
&\eqsim \begin{pmatrix} 0 & I \end{pmatrix} A^{(k)} (A^{(k)} + X)^{-1} A^{(k)} \begin{pmatrix} 0 \\ I \end{pmatrix} \\
&= \underbrace{\begin{pmatrix} 0 & I \end{pmatrix} A^{(k)} \begin{pmatrix} 0 \\ I \end{pmatrix}}_{= A_{\Delta\Delta}^{(k)}} - \begin{pmatrix} 0 & I \end{pmatrix} A^{(k)} (A^{(k)} + X)^{-1} X \begin{pmatrix} 0 \\ I \end{pmatrix},
\end{aligned}$$

where $X := H_k^{-4} M^{(k)} \underline{e}_h \underline{e}_h^\top M^{(k)}$ and $M^{(k)}$ is the mass matrix on the physical patch. From $(A^{(k)} + X)\underline{e}_h = 0 + H_k^{-4} M^{(k)} \underline{e}_h \underline{e}_h^\top M^{(k)} \underline{e}_h = |\Omega^{(k)}| H_k^{-4} M^{(k)} \underline{e}_h$ we obtain $(A^{(k)} + X)^{-1} M^{(k)} \underline{e}_h = |\Omega^{(k)}|^{-1} H_k^4 \underline{e}_h$. In total, we obtain

$$A_{\Delta\Delta}^{(k)} P^{(k)} A_{\Delta\Delta}^{(k)} \eqsim A_{\Delta\Delta}^{(k)} - |\Omega^{(k)}|^{-1} H_k^4 \begin{pmatrix} 0 & I \end{pmatrix} \underbrace{A^{(k)} \underline{e}_h}_{= 0} \underline{e}_h^\top M^{(k)} \begin{pmatrix} 0 \\ I \end{pmatrix},$$

which finishes the proof. □

Let $B_\Delta := (B_\Delta^{(1)}, \ldots, B_\Delta^{(K)})$. Using algebraic reformulations and Lemma 3.1, it follows that the approximate Schur complement matrix $\widehat{F} = B_\Delta P B_\Delta^\top + B_\Pi A_\Pi^{-1} B_\Pi^\top$ is spectrally equivalent to the IETI-DP matrix F from [10].

An analogous statements holds for the scaled Dirichlet preconditioner $M_{\mathrm{sD}} = B_\Gamma D^{-1} S D^{-1} B_\Gamma^\top$ and $\widehat{M}_{\mathrm{sD}} = B_\Gamma D^{-1} \widehat{S} D^{-1} B_\Gamma^\top$ by using the fact that $\widehat{S}^{(k)}$ and $S^{(k)}$ represent discrete harmonic extensions, i.e., the extensions that minimize the

energy norm and the norm equivalence, [10, Lemma 4.13], again applicable because of (2).

The following theorem shows that the use of our proposed preconditioner P does not degrade the qualitative behavior of the condition number estimate from [10, Theorem 4.1] for the overall system.

Theorem 3.2. *Under the presented assumptions, the condition number of the system* (6) *preconditioned with* (7) *is bounded by*

$$C\,p\,\left(1+\log p+\max_{k=1,\dots,K}\log\frac{H_k}{h_k}\right)^2,$$

where the constant C only depends on the constant C_G, the quasi-uniformity constant (see [10, Ass. 4]) and the maximum number of patches sharing a vertex (see [10, Ass. 3]).

Proof. All constants in this theorem are positive and only depend on the abovementioned constants. Using [8, Theorem 22] and [10, Theorem 4.1], we have

$$\sigma(M_{\mathrm{sD}}F)\subseteq\left[1,p\left(1+\log p+\max_{k=1,\dots,K}\log\frac{H_k}{h_k}\right)^2\overline{\sigma}_1\right]$$

for some constant $\overline{\sigma}_1$. Using the equivalences $F\eqsim\widehat{F}$ and $M_{\mathrm{sD}}\eqsim\widehat{M}_{\mathrm{sD}}$, we obtain

$$\sigma(\widehat{M}_{\mathrm{sD}}\widehat{F})\subseteq\left[\underline{\sigma}_2,p\left(1+\log p+\max_{k=1,\dots,K}\log\frac{H_k}{h_k}\right)^2\overline{\sigma}_2\right] \tag{8}$$

for constants $\underline{\sigma}_2$ and $\overline{\sigma}_2$. Using Lemma 3.1, we get

$$\sigma(PA_{\Delta\Delta})\subseteq[\underline{\sigma}_3,\overline{\sigma}_3], \tag{9}$$

where $A_{\Delta\Delta}:=\mathrm{diag}\,(A^{(1)}_{\Delta\Delta},\dots,A^{(K)}_{\Delta\Delta})$, with some constants $\underline{\sigma}_3$ and $\overline{\sigma}_3$. The theorem of Brezzi, cf. [1], in combination with (8) and (9) concludes the proof. □

3.2 Analysis of the system for the primal basis

In this subsection, we show a condition number result that guarantees that the local MINRES solvers required to obtain the local bases $\Psi^{(k)}$ can be realized with a computational cost that does not exceed the complexity of the main iteration. First, we need to show an auxiliary lemma.

Lemma 3.3. *Let $\widehat{u}$ be a B-spline function of degree p over a quasi uniform grid on $\widehat{\Omega}$ with grid size $\widehat{\Omega}$ and assume that $\widehat{u}(0)=0$. Then,*

$$\left(\int_{\widehat{\Omega}}\widehat{u}(x)\mathrm{d}x\right)^2\lesssim\left(1+\log p+\log\frac{1}{\widehat{h}}\right)|\widehat{u}|^2_{H^1(\widehat{\Omega})}.$$

Proof. We decompose $\widehat{u} = \widehat{u}_0 + c$ such that $\int_{\widehat{\Omega}} \widehat{u}_0(x)\,\mathrm{d}x = 0$ and $c = \int_{\widehat{\Omega}} \widehat{u}(x)\,\mathrm{d}x \in \mathbb{R}$. [10, Lemma 4.14] yields

$$|\widehat{u}_0(0)|^2 \lesssim \left(1 + \log p + \log \frac{1}{\widehat{h}}\right) \|\widehat{u}_0\|^2_{H^1(\widehat{\Omega})}.$$

Using Poincaré's inequality, we obtain

$$|\widehat{u}_0(0)|^2 \lesssim \left(1 + \log p + \log \frac{1}{\widehat{h}}\right) |\widehat{u}_0|^2_{H^1(\widehat{\Omega})} = \left(1 + \log p + \log \frac{1}{\widehat{h}}\right) |\widehat{u}|^2_{H^1(\widehat{\Omega})}.$$

$\widehat{u}(0) = 0$ implies $|\widehat{u}_0(0)| = |c| = |\int_{\widehat{\Omega}} \widehat{u}(x)\,\mathrm{d}x|$, which finishes the proof. □

Theorem 3.4. *For $k = 1, \dots, K$, the condition number of $\widetilde{P}^{(k)}\widetilde{\mathcal{A}}^{(k)}$ is bounded by*

$$C\left(1 + \log p + \log \frac{H_k}{h_k}\right),$$

where the constant C only depends on the constant C_G and the quasi-uniformity constant (see [10, Ass. 4]).

Proof. We prove this equivalence by showing that the assumptions of Brezzi's theorem [1] are satisfied. By the norm equivalence [10, Lemma 4.13], we obtain $A^{(k)} \eqsim \widehat{A}^{(k)}$. In the kernel of $C^{(k)}$, we use Lemma 3.3 to obtain the equivalence $A^{(k)} \eqsim \widehat{A}^{(k)} \eqsim \widehat{A}^{(k)}_M$. This kernel coercivity and the boundedness assumptions on $A^{(k)}$ are satisfied. The remaining inf-sup and boundedness conditions are trivially fulfilled due to the use of a Schur complement preconditioner. Hence, the statement of the theorem follows. □

4 Numerical results

In this section, we show numerical results of the proposed inexact IETI-DP method for the computational domains as given in Fig. 1. The first domain is a quarter annulus consisting of 32 patches and the second one is the Yeti-footprint decomposed into 84 patches.

We consider the model problem

$$-\Delta u(x, y) = 2\pi^2 \sin(\pi x) \sin(\pi y) \quad \text{for} \quad (x, y) \in \Omega$$

with homogeneous Dirichlet boundary conditions. Within each patch, we use B-splines of degree p and maximum smoothness C^{p-1}. The coarsest discretization space ($r = 0$) is the space of patchwise global polynomials, only the more rectangular patches of the Yeti-footprint have one inner knot on each of the longer sides of the patches. The subsequent refinements $r = 1, 2, \dots$ are obtained via uniform refinement steps.

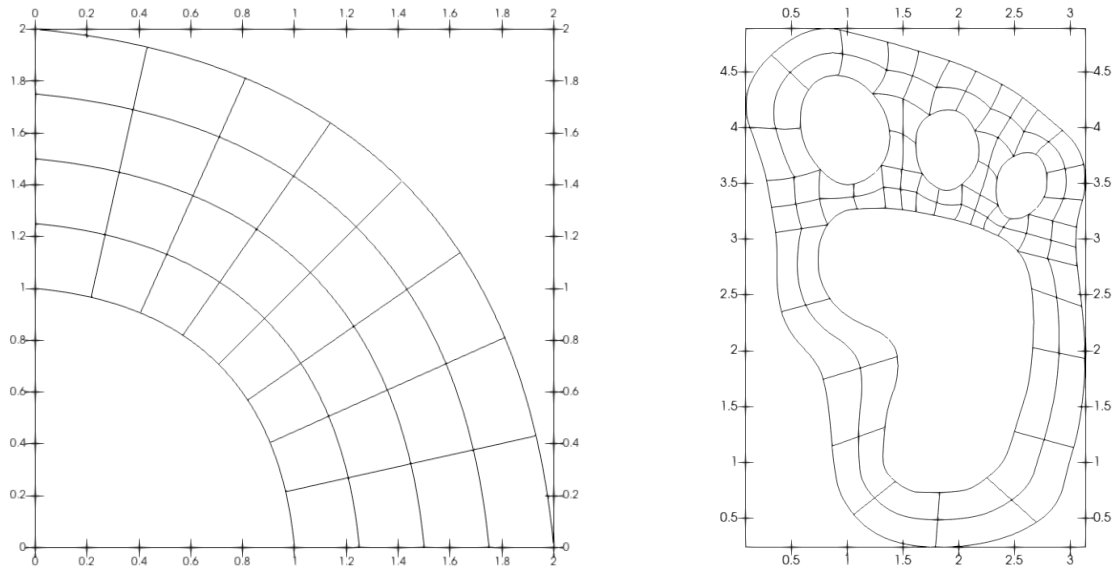

Figure 1: Computational domains; Quarter annulus (left); Yeti-footprint (right)

All numerical experiments have been carried out using the C++ library G+Smo[1], the CPU times have been recorded on the Radon1[2] Cluster in Linz.

We compare three different IETI-DP solvers: the proposed solver as introduced in Section 2 (=MFD), a IETI-DP solver for the saddle point system (6) without the primal degrees of freedom eliminated with direct solvers for the local subproblems (=MLU), and the Schur complement based approach as introduced in [10] (=CGLU). We use MINRES as outer solver in the cases MFD and MLU and conjugate gradient as outer solver for the case CGLU. For MLU and CGLU, we use sparse direct LU solvers from the Pardiso project[3] for the local subproblems and for computing the bases $\Psi^{(k)}$. We start all numerical experiments with zero initial guess and stop the iterations if the ℓ_2-norm of the residual vector is reduced by a factor of 10^{-6} compared to the ℓ_2-norm of the right-hand side vector. For MFD, the primal bases $\Psi^{(k)}$ are solved with MINRES up to an accuracy of 10^{-8}.

In the Tables 1 and 2, we present the timings of the algorithms on the quarter annulus domain. The time required for computing the primal basis Ψ is indicated with the same letter. The accumulated setup and application times of the different local preconditioners for all patches K are indicated by Θ_S and Θ_A, respectively. Moreover, we present the overall solving times and the number of iterations (it.) required by the main Krylov space solver.

We observe that the solving and total times required by MFD are three to five times smaller compared to the other methods MLU and CGLU. MFD is much faster than

[1] `https://github.com/gismo/gismo`
[2] `https://www.ricam.oeaw.ac.at/hpc/`
[3] `https://www.pardiso-project.org/`

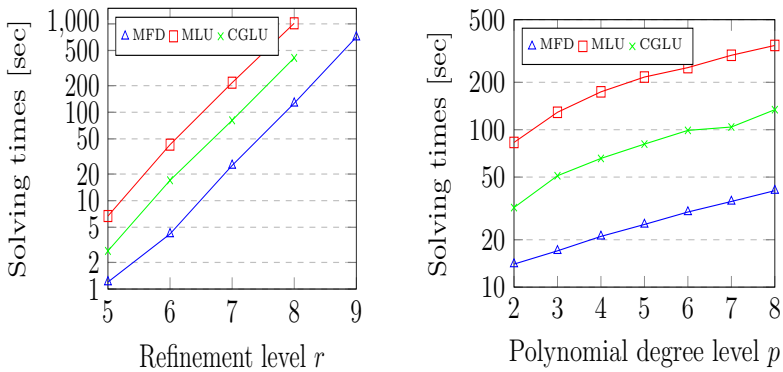

Figure 2: Solving times for $p = 5$ (left) and $r = 7$ (right); MFD (blue lines); MLU (red lines); CGLU (green lines); Quarter annulus

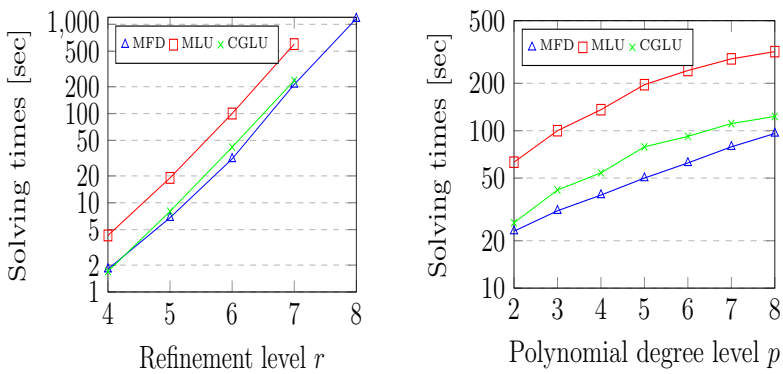

Figure 3: Solving times for $p = 3$ (left) and $r = 6$ (right); MFD (blue lines); MLU (red lines); CGLU (green lines); Yeti-footprint

the other methods despite the fact that the required number of iterations are up to approximately six times larger. One disadvantage of MFD is the computation of the primal basis Ψ. The tables show a larger computation time when using MFD. This is a weakness of the classical preconditioned MINRES method when applied to problems with multiple right-hand sides. In general, we have to solve systems with four right-hand sides to compute $\Psi^{(k)}$. Moreover, we see that the setup and application of the FD based preconditioner is much faster compared to the factorization of the matrices $\widetilde{A}^{(k)}$ and the application of these factorizations. Table 2 shows another advantage of the MFD method. Since its memory footprint is smaller, it also provides a solution vector to the considered linear system for the refinement level $r = 8$. The plots in Fig. 2 visualize solving times of the IETI-DP solvers on the quarter annulus domain. We mark the performance of MFD with blue lines and triangles, MLU with red lines and squares and the performance of CGLU is indicated with green lines and crosses. In both graphs, we observe that MFD is the fastest algorithm. In the left plot, we see

	r	Ψ	Θ_S	Θ_A	solving	total	it.
MFD	6	1.2	0.1	0.4	4.2	5.5	71
MLU		0.8	7.6	21.2	43.0	51.4	37
CGLU		0.8	7.6	9.5	17.0	15.4	15
MFD	7	8.0	0.3	4.9	25.0	33.3	80
MLU		4.0	42.3	106.4	216.0	262.3	39
CGLU		4.0	42.3	45.4	81.0	127.3	15
MFD	8	35.5	2.0	26.9	126.3	163.8	88
MLU		18.1	243.6	503.8	1015.0	1276.7	41
CGLU		18.0	242.1	225.3	412.0	672.1	17

Table 1: Alg. A; $p = 5$; timings in sec.; Quarter annulus

	r	Ψ	Θ_S	Θ_A	solving	total	it.
MFD	6	2.5	0.2	0.5	8.2	10.9	76
MLU		1.2	17.9	33.8	72.0	91.1	39
CGLU		1.2	17.8	14.4	26.0	45.0	15
MFD	7	15.1	0.4	5.4	41.0	56.5	84
MLU		5.8	105.0	163.3	343.0	453.8	41
CGLU		5.8	105.0	73.8	134.0	244.8	17
MFD	8	60.1	2.3	29.9	200.0	262.4	94
MLU				OoM			
CGLU				OoM			

Table 2: Alg. A; $p = 8$; timings in sec.; Quarter annulus

that for spline degree $p = 5$, the solving times increase rather linearly with respect to the number of unknowns. Moreover, the left graph shows that MFD computes the solution for the linear system even for refinement level $r = 9$ (≈ 8.5M dofs). In the right graph, we present the solving times with respect to the spline degree for refinement level $r = 7$. The solving times for the three IETI-DP solvers increase about linearly with the spline degree.

The plots in Fig. 3 show solving times of the IETI-DP solvers on the Yeti-footprint. We marked the performance of the different IETI-DP solvers as above in the experiments on the quarter annulus. The plot on the left shows the increase of the solving time with respect to the refinement level with polynomial degree $p = 3$ and the plot on the right shows the increase of the solving time with respect to the polynomial degree, where we have fixed the refinement level to $r = 6$. As for the quarter annulus, we see that MFD is superior compared to MLU and CGLU also on the Yeti-footprint with respect to the solving times and the smaller memory footprint of MFD allows us to consider larger problems. In both plots, we observe similar growth rates of the solving time for all three solvers as in Fig. 2. In the Tables 3 and 4, we present and compare the required timings for the polynomial degrees $p = 3$ and $p = 7$ for different

	r	Ψ	Θ_S	Θ_A	solving	total	it.
MFD	5	0.7	0.1	0.8	6.8	7.6	213
MLU		0.3	2.3	9.4	19.0	21.6	45
CGLU		0.3	2.3	4.5	8.0	10.6	20
MFD	6	3.4	0.2	5.0	31.0	34.6	242
MLU		1.2	10.5	49.6	100.0	111.7	51
CGLU		1.2	10.4	23.1	42.0	53.6	22
MFD	7	21.8	1.2	52.7	212.0	235.0	274
MLU		6.8	50.3	295.2	600.5	657.6	55
CGLU		6.8	50.1	126.1	234.0	290.9	22

Table 3: Alg. A; $p = 3$; timings in sec.; Yeti-footprint

	r	Ψ	Θ_S	Θ_A	solving	total	it.
MFD	5	2.2	0.2	1.2	20.0	22.4	249
MLU		0.6	10.5	23.5	48.0	59.1	51
CGLU		0.6	10.4	10.9	19.0	30.0	22
MFD	6	9.5	0.4	5.9	79.0	88.9	282
MLU		3.0	44.8	140.5	286.0	333.8	57
CGLU		3.0	44.8	60.6	111.0	158.8	23
MFD	7	54.2	1.5	63.2	414.0	469.7	309
MLU		14.1	265.3	739.1	1521.0	1800.4	61
CGLU		13.8	261.7	304.4	570.0	845.5	25

Table 4: Alg. A; $p = 7$; timings in sec.; Yeti-footprint

refinement levels for the Yeti-footprint.

To conclude, we presented a fast IETI-DP method which allows the incorporation of inexact solvers for the local subproblems while maintaining the condition number bound as established in [10]. It is beneficial both because of its smaller memory footprint and its faster convergence for the model problems.

Acknowledgments. The first author was supported by the Austrian Science Fund (FWF): S117-03 and W1214-04. Also, the second author has received support from the Austrian Science Fund (FWF): P31048.

References

[1] F. Brezzi. On the existence, uniqueness and approximation of saddle-point problems arising from lagrangian multipliers. *ESAIM: Math. Model. Numer. Anal.*, 8(R2):129 – 151, 1974.

[2] C. Farhat, M. Lesoinne, P. L. Tallec, K. Pierson, and D. Rixen. FETI-DP: A dual-primal unified FETI method I: A faster alternative to the two-level FETI method. *Int. J. Numer. Methods Eng.*, 50:1523 – 1544, 2001.

[3] C. Hofer and U. Langer. Dual-primal isogeometric tearing and interconnecting solvers for multipatch continuous and discontinuous Galerkin IgA equations. *PAMM*, 16(1):747–748, 2016.

[4] C. Hofer, U. Langer, and S. Takacs. Inexact Dual-Primal Isogeometric Tearing and Interconnecting Methods. In P. E. Bjørstad, S. C. Brenner, L. Halpern, H. H. Kim, R. Kornhuber, T. Rahman, and O. B. Widlund, editors, *Domain Decomposition Methods in Science and Engineering XXIV*, pages 393–403. Springer International Publishing, 2018.

[5] T. J. R. Hughes, J. A. Cottrell, and Y. Bazilevs. Isogeometric analysis: CAD, finite elements, NURBS, exact geometry and mesh refinement. *Comput. Methods Appl. Mech. Eng.*, 194(39-41):4135 – 4195, 2005.

[6] A. Klawonn and O. Rheinbach. Inexact FETI-DP methods. *Int. J. Numer. Methods Eng.*, 69(2):284 – 307, 2007.

[7] S. Kleiss, C. Pechstein, B. Jüttler, and S. Tomar. IETI-Isogeometric Tearing and Interconnecting. *Comput. Methods Appl. Mech. Eng.*, 247-248:201 – 215, 2012.

[8] J. Mandel, C. R. Dohrmann, and R. Tezaur. An algebraic theory for primal and dual substructuring methods by constraints. *Appl. Numer. Math.*, 54(2):167 – 193, 2005.

[9] G. Sangalli and M. Tani. Isogeometric preconditioners based on fast solvers for the Sylvester equation. *SIAM J. Sci. Comput.*, 38(6):A3644 – A3671, 2016.

[10] R. Schneckenleitner and S. Takacs. Condition number bounds for IETI-DP methods that are explicit in h and p. *Math. Models Methods Appl. Sci.*, 30(11):2067–2103, 2020.